ARTICLE NO. 78-1002R

A80-038

Solving Subsynchronous Whirl in the High-Pressure Hydrogen Turbomachinery of the SSME

Matthew C. Ek*
Rockwell International/Rocketdyne Division, Canoga Park, Calif.

The high-pressure turbomachinery for the Space Shuttle Main Engine (SSME) has the highest power-to-weight ratio known. Subsynchronous shaft whirl of the high-pressure fuel turbopump (77,000 hp, 760 lb) limited operation of the SSME for some months in early 1976. The means by which this problem was successfully attacked is presented herein. The principal forcing functions of the phenomena were adjudged to be turbine cross-coupling and interstage seal effects in combination with low-system stiffness and damping. The whirl inception speed and the first-shaft critical speed were increased by stiffening the shaft and bearing supports. System damping and stiffness were additionally augmented by utilizing the interstage seals as axial flow hydrodynamic bearings. The instability threshold speed is now greater than the operating speed at rated engine thrust.

Nomenclature

C = effective support damping, lb-s/in.
C_{xx}, C_{yy} = seal damping, lb-s/in.
C_{xy}, C_{yx} = seal cross-coupled damping, lb-s/in.
D = bore diameter, mm
DN = rolling element bearing parameter
D_p = turbine blade pitch diameter, in.
F_x = force on shaft in x direction, lb
F_y = force on shaft in y direction, lb
H = turbine blade height, in.
K = stiffness, lb/in.
K_B = bearing stiffness, lb/in.
K_E = total equivalent support stiffness, lb/in.
K_S = bearing carrier stiffness, lb/in.
K_t = turbine cross-coupled spring rate, lb/in.
K_x, K_y = bearing support spring rates in x,y directions, lb/in.
K_{xx}, K_{yy} = seal spring rates, lb/in.
K_{xy}, K_{yx} = seal cross-coupling spring rates, lb/in.
N = shaft speed, rpm
N_n = shaft critical speeds (n = order of critical speed = 1,2,3...), rpm
α = nonlinear coefficient on radial deflection, in.$^{-2}$
β = "Alford" coefficient: $K_t = \tau\beta/D_pH$,

$$\begin{Bmatrix} F_x \\ F_y \end{Bmatrix} = \begin{bmatrix} 0 & K_t \\ -K_t & 0 \end{bmatrix} \begin{Bmatrix} X \\ Y \end{Bmatrix}$$

ϵ_e = external damping, lb-s/in.
ϵ_i = internal, or rotor, damping of system, lb-s/in.
ω = shaft speed, Hz or rad/s
$\omega_{cr} = \Omega_o$ = first system critical speed, Hz or rad/s
ω_D = shaft speed at "dropout" (whirl ceases), Hz or rad/s
ω_I = shaft speed at "inception" (whirl begins), Hz or rad/s
Ω = rate of whirl, Hz or rad/s
τ = torque, lb-in.
ξ = ratio of damping to critical damping

Presented as Paper 78-1002 at the AIAA/SAE 14th Joint Propulsion Conference, Las Vegas, Nev., July 25-27, 1978; submitted Oct. 23, 1978; revision received Sept. 5, 1979.

Index categories: Rotating Machinery; Liquid Rocket Engines and Missile Systems; Structural Stability.

* Professor of Engineering, University of California at Northridge; formerly Vice President, Engineering & Test, Rockwell International.

Introduction

THE Space Shuttle Main Engine (SSME) is a liquid oxygen/hydrogen topping cycle rocket engine presently being developed by the Rocketdyne Division of Rockwell International as the main propulsor for the Space Shuttle. It is designed to develop approximately 470,000 lb of thrust in vacuo with 455.2 s of specific impulse at a chamber pressure of 2960 psia to achieve rated power level (RPL), or 512,000 lb vacuum thrust and 3240 psia at full power level (FPL), and to be throttled to 50% thrust if required. Due to the constraints of the cycle, four turbopumps are employed, the two high-pressure pumps having the highest power-to-weight ratio known. In particular, the high-pressure fuel turbopump (HPFTP) is rated at FPL at approximately 76,000 hp with a weight of 760 lb. The turbomachinery design constraints and objectives have been delineated by Rothe,[1] and general turbomachinery operating conditions are exhibited in Table 1. Pertinent design features of the HPFTP will now be addressed.

Description of the HPFTP

An expanded and separated half cross section of the HPFTP with the principal areas of interest highlighted is shown in Fig. 1. The relationship of static to rotating elements, the seal areas of interest, and the bearing arrangements are shown.

The rotor weighs approximately 130 lb and is of built-up construction with three impellers (12-in. diameter) and two turbine wheels (11-in. diameter) tightly clamped together on piloted splined collars by a central drawbolt. This arrangement was dictated by the necessity of holding the eye diameter of the impeller to a minimum for optimum specific speed and minimizing the tip diameter of the impeller for stress reasons. This approach mandated a large number of pilot diameter and splines. The rotor is positioned radially by two sets of individually spring-loaded 45-mm hydrogen-cooled duplex ball bearings. These are free to slide axially on the outside diameter of the outer races in the casing bearing carriers. The rotor is positioned axially by a thrust bearing at the pump end for start transients (disengages at ~12,000 rpm) and a self-referencing balance piston (the back surface of the third stage impeller) for normal operation.

There are a number of sealing diameters between rotor and stator, shown in Fig. 1 as nos. 1-12; nos. 1-9 are liquid hydrogen close clearance seals with various pressure drops,

Table 1 SSME design data at rated power level

Thrust chamber parameters	
Nozzle stagnation pressure	= 2960 psia
Oxidizer flowrate	= 888 lb/s
Fuel flowrate	= 148 lb/s

Turbomachinery	Low pressure		High pressure		
	Oxidizer	Fuel	Oxidizer Main stage	Oxidizer Boost stage	Fuel
Pump					
Inlet flowrate, lb/s	888	148	1070	86	148
Inlet pressure, psia	100	30	467	4633	281
Discharge pressure, psia	467	281	4290	6957	6000
Efficiency	0.70	0.66	0.68	0.76	0.76
Turbine					
Inlet pressure, psia	4115	4350	5000		4900
Inlet temperature, *R*	192	544	1550		1790
Pressure ratio	8.8	1.20	1.50		1.47
Efficiency	0.62	0.55	0.75		0.79
Speed, rpm	5100	16,000	27,500		34,700
Horsepower	1470	2800	25,000		61,000

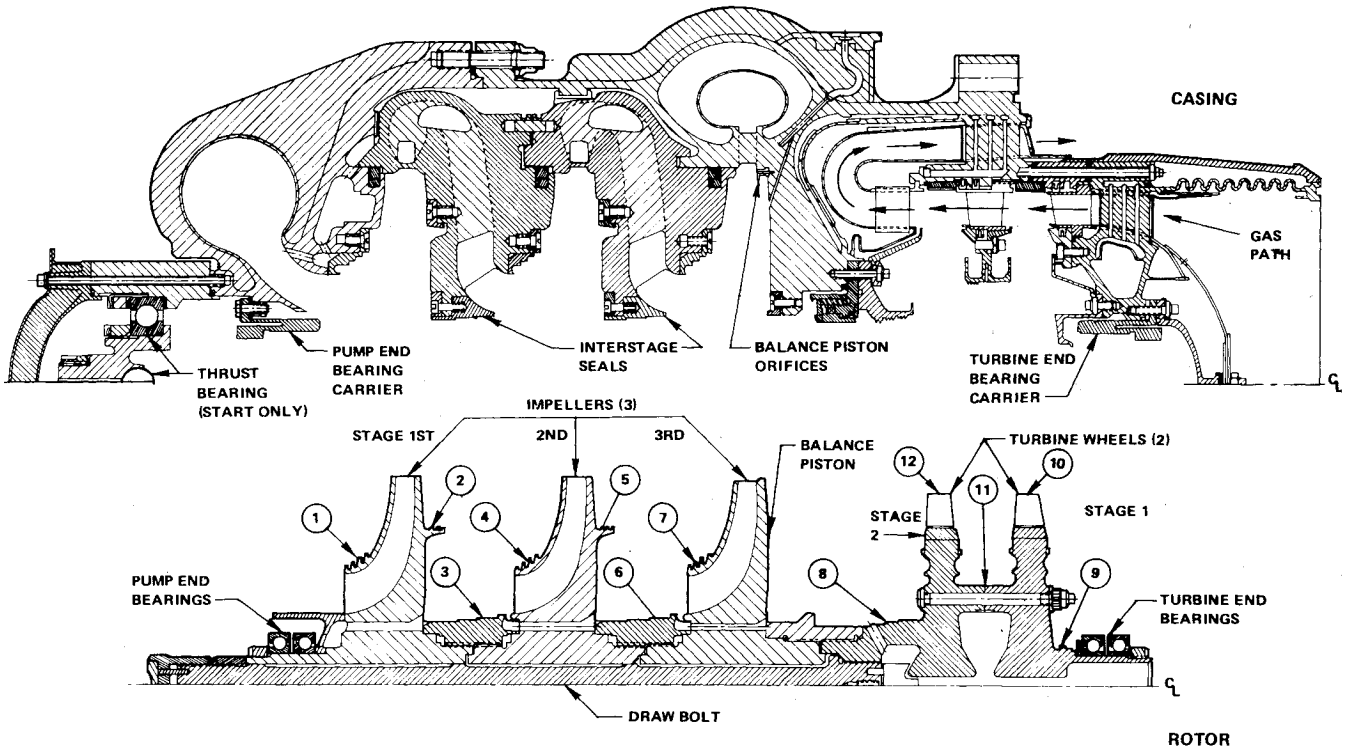

Fig. 1 Half cross section of high-pressure fuel turbopump.

while nos. 10-12 seal gaseous hydrogen or preburner products (steam and gaseous hydrogen) at various temperatures. These seals are of particular importance because of their effect on the dynamic environment of the rotor.

The rotor was designed to operate dynamically between the second and third critical speeds (Fig. 2) with the operating range as shown. This was accomplished by utilizing a flexible cage bearing support, lightly damped by a Belleville spring axially loaded at each end to provide friction (see Fig. 3, no. 1, Basic Design). The low (150,000 lb/in.) spring rate of this flexible bearing support ensured that the machine would run through the first two critical speeds at low rpm.

An outboard turbine bearing is utilized to hold bearing *DN* to a minimum. An overhung turbine would have necessitated a large diameter (90 mm) bearing between turbine and pump with a *DN* of approximately 3.4×10^6. Prior experience was at a limit of 2.2×10^6. This decision contributed to rotor flexibility by increasing the span between bearings.

A dynamic constraint peculiar to liquid hydrogen turbopumps is implicit in the very low viscosity of this medium ($\mu \approx 1.5 \times 10^{-9}$ lb-s/in.^{2}), the fact that it is cryogenic, and the low density (4.42 lb/ft^3). These preclude the incorporation of any ordinary or practical squeeze film dampers in the machine and results in very light system damping derived from the pumped medium.

Description of Problem and Initial Test Results

Early in the development program, considerable vibration and accelerometer activity at frequencies other than synchronous were noted on the HPFTP, both in component testing and in the engine. The significance of these data was not fully appreciated at first because of the existence of a

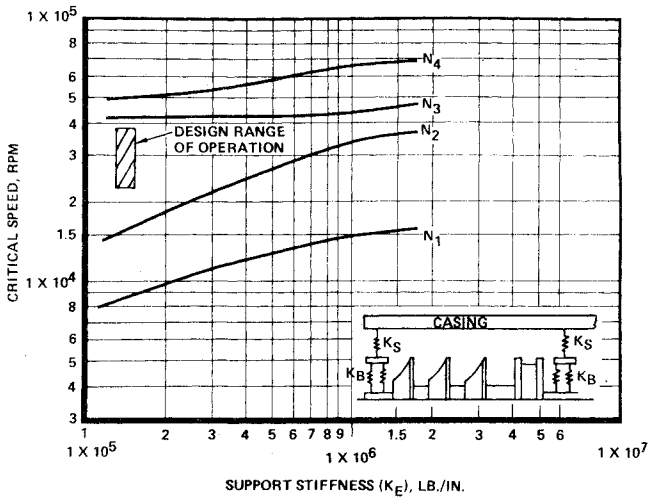

Fig. 2 Undamped critical speeds vs effective support stiffness (original baseline design).

persistent axial balance piston problem which masked the subsynchronous phenomenon. When the balance piston problem was resolved and engine testing at increasing power levels was resumed, the nonsynchronous vibration problem became acute at speeds above 19,000 rpm, to the extent of causing turbine bearing failures. The characteristics of the vibration were remarkably consistent. Also, they were marked by a forward precession of the shaft at less than shaft speed with bearing loads rapidly increasing a nonlinear manner at a frequency typically 0.5-0.56 of the shaft speed until a destructive limit cycle was attained. The phenomenon was identified as subsynchronous whirl and became characteristically more violent as higher speeds were attempted. Accelerometer cutoff was common for any speed in excess of 22,000 rpm. Location of accelerometers on the machine is shown in Fig. 4, and typical dynamic data are shown in Fig. 5. Inception of the whirl phenomenon was very rapidly followed by a buildup in amplitude and frequency as the bearing supports bottomed out under increased bearing load and the critical speed of the system increased nonlinearly. In this case, the inception occurred at a shaft speed of approximately twice the first critical speed, and the whirl frequency thereafter followed the critical speed of the system at approximately one-half the shaft speed. Radial and axial accelerometers and pressure measurements were in phase, which led to early speculation of a possible axial forcing function or coupled instability involving the balance piston. Upon engine cutoff, the nonlinearity of the system was further emphasized by a dropout from the subsynchronous phase at a lower speed than the inception. This type of behavior in nonlinear systems has been widely noted in the literature; for example, Hori,[2] Kushul',[3] and Bolotin.[4]

Shaft and bearing deflections and loads were high enough to cause interferences at sealing surfaces, wear rings, and turbine blades and resulted in fretting at some pilot diameters. A significant number of very rapid (in some cases a few seconds) turbine bearing failures occurred with estimated turbine bearings loads of approximately 10 times the desirable limit. Turbine end bearing loads were much larger than pump end bearing loads as inferred from bearing tracks and casing model analysis, and in no case was there a pump end bearing failure.

Gunter[5] termed this example as "the most violent case in his experience."

Prior Experience

Of eight other government-sponsored programs involving liquid hydrogen turbomachinery, four exhibited some degree of subsynchronous whirl. Those showing symptoms of varying degrees of severity were early versions of the Mark 15 J-2, the Mark IX turbopump for the Rover program, the Mark 25 turbopump for the Phoebus program, and the 350K high-pressure pump developed by Pratt & Whitney. In the

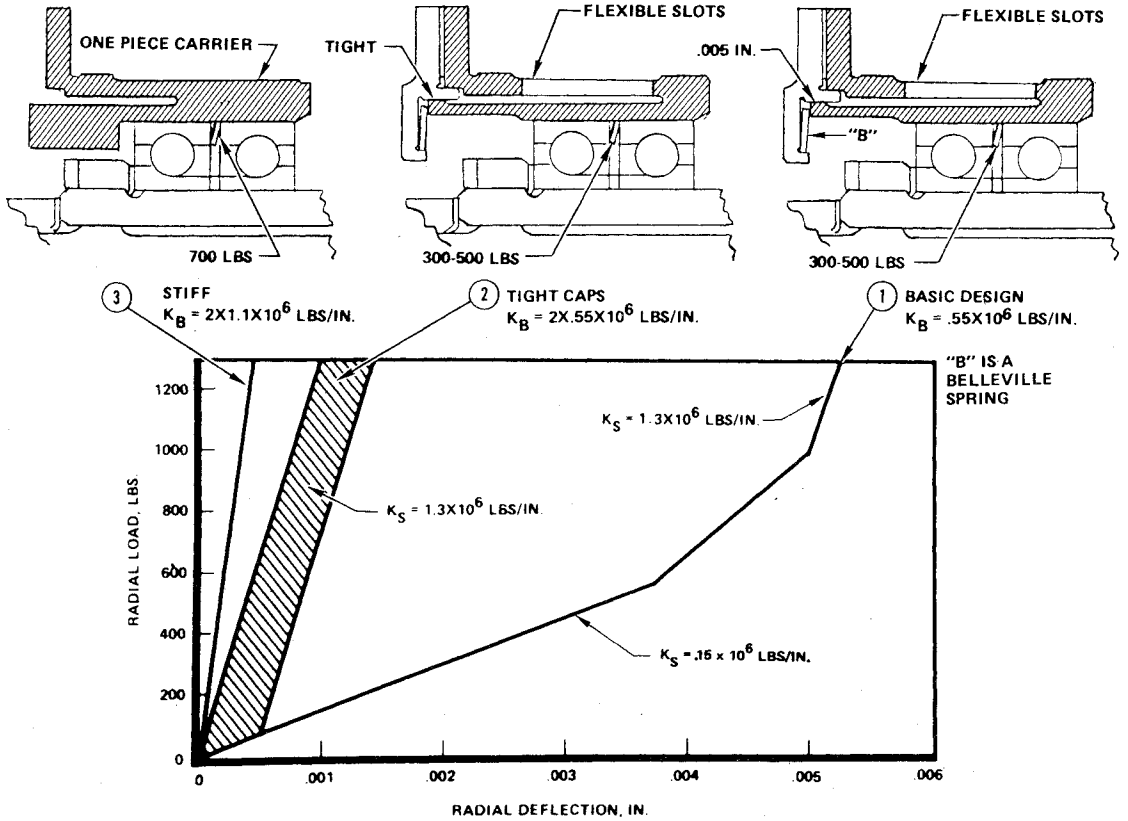

Fig. 3 HPFTP effective support stiffness for various bearing carrier configurations.

Table 2 Possible contributors to instability

Possible "drivers"	Authorities	Behavior
Rotor internal hysteresis or damping	Newkirk, Gunter, Ehrich, Tondl, Kushul', Bolotin, et al.	Dependent on system
Seals (journal bearing similarities)	Poritsky, Haag, Black, Hori, and Childs	$\omega_I = \Omega_o (1+\epsilon_e/\epsilon_i)$, $\Omega_o = \omega_{cr}$ $\Omega \leq \omega/2$, $\omega_I \leq 2\Omega_o$
Alford effect (aerodynamic cross-coupling)	Alford (G.E.), et al.	$\Omega = \Omega_o$
Axial-radial coupling	Bolotin, Mathieu, Den Hartog, et al.	$\Omega = \omega/2$
Impeller/diffuser interaction	Black	$\Omega = \Omega_o$
Nonlinear support	Billett	$\omega^2 = \Omega_o{}^2 (1+aR^2)(1+\epsilon_e/\epsilon_i)^2$
Degree of rotor balance	Kushul' and Tondl	$\omega_I > 2\Omega_o$, $\omega_D < \omega_I$
Pulsating torque	Eshelmann	$\Omega = n\omega/2$ $(n = 1,2,3)$
Fluid in rotor	Ehrich	$\omega/2 < \Omega < \omega$

case of the Mark 15 J-2, increasing bearing preload was sufficient to eliminate the problem. Stiffening of the bearings by means of incorporation of a duplex package, or higher bearing preload in conjunction with balance piston adjustments, stabilized the design for the Mark 25 and Mark IX pumps. In the case of the 350K turbopump, considerable stiffening of the bearing package with a consequent substantial increase in the system's first and second critical speeds was necessary to completely solve the problem (see Ref. 6). As a result of this review, it appeared that as power increased per unit weight in lightly damped machines, such as liquid hydrogen turbomachinery, the susceptibility of a machine to cross-coupling effects was exacerbated. Additional possible correlations emerged with regard to whether the turbine was or was not shrouded, with unshrouded turbine blades being more susceptible, whether built-up rotors were used, and whether a large number of sealing points and pilot diameters were inherent in the design.

Although the HPFTP design incorporated the best design features from prior programs, at the time that the machine was designed (1970) there was insufficient understanding of the subsynchronous whirl phenomenon in high-power liquid hydrogen turbomachinery, particularly in the understanding of the forcing functions, to accurately predict the existence of a whirl problem. Significantly, however, Childs,[7] utilizing some recently developed seal coefficients (due to Black[8-18]), hypothesized in 1975 the possibility of an instability due to interstage seal effects in the neighborhood of 20,000 rpm or above.

Literature

Behavior of rotating machinery in a subsynchronous whirl manner is referred to in a wide variety of literature,[19-33] and many companies engaged in the manufacture of rotating machinery have encountered it in some form. Additionally, behavior and analysis of distinctly nonlinear phenomena are dealt with in a number of references, e.g., Refs. 2-4. With very few exceptions, however, analytical references deal with simple systems with single "drivers" (destabilizing cross-coupling influences) and simple linear systems for response. Definition of cross-coupling possibilities, such as seals, bearings, internal hysteresis in shafting, etc., is dealt with in the literature as isolated phenomena. In this case, a great deal of complication was inevitable as a result of the presence of multiple drivers and the certainty of nonlinear behavior of both drivers and response.

Of 22 possible drivers in the machine identified from all sources of information, 9 of the most likely were hypothesized (see Yu[34] and Table 2) together with the expected behavior for each phenomenon applied individually.

Analytical Approach and Mathematical Models

To define critical parameters and to duplicate the phenomenon, five separate mathematical models were constructed. It was recognized at the outset that the only models which would give results with any degree of certainty would be those with relatively simple combinations of linear approximations, while nonlinear models, taking into account many more factors, would take a longer period of time to produce any quantitative output and would run the risk of never producing reliable and usable solutions. The five models are described as follows:

Table 3 Seal characteristics at rated power level

Seal location (Ref: Fig. 1)	$K_{xx} = K_{yy}$	K_{yz}	C_{xx}	C_{yx}
1	2100	740	0.4	...
2	5900	1700	0.93	...
3	13,000	13,000	7.1	0.3
4	2500	850	0.47	...
5	7800	2000	1.07	...
6	15,200	14,000	7.7	0.3
7	3000	930	0.51	...
8	1200	1200	0.7	...
9	200	400	200	...
11	7	65	...	...

1) A digital linear stability model was progressively evolved at the University of Louisville, Kentucky, by Childs.[35] This model had predicted a possible instability as early as 1975 and was refined as test data became available.

2) A digital linear stability model was constructed by Gunter and associates[5] in 1976 at the University of Virginia. Many refinements were incorporated, including additional personal inputs by Black[8-18] on seal representation.

3) A digital nonlinear time domain model with a multitude of nonlinear effects was constructed at Rocketdyne by Rowan[34,36] in 1976.

4) A digital nonlinear time domain stability model, including axial-radial coupling considerations, was constructed at MSFC by Goetz et al.[37].

5) An analog hybrid nonlinear model in real time was constructed by Thompson et al.[33] at Rocketdyne.

A description of some of the key factors incorporated in the models will now be addressed.

General

All models included damping at the bearing supports, the ability to handle asymmetrical bearing support effects, interstage hydrogen seal forces, a flexible casing of some description, turbine cross-coupling (the Alford effect), the ability to predict bearing loads, and the ability to incorporate predicted unbalance in the rotating parts. Most models assumed that the low frequency of the pump casing/engine connection (45-100 Hz) allowed the assumption of a stationary engine. Detailed summaries of the fundamental dynamic equations involved are very competently dealt with in published and unpublished work by Gunter,[5] Childs,[35] Rowan,[36] Thompson and Sack,[34] and Worley.[37]

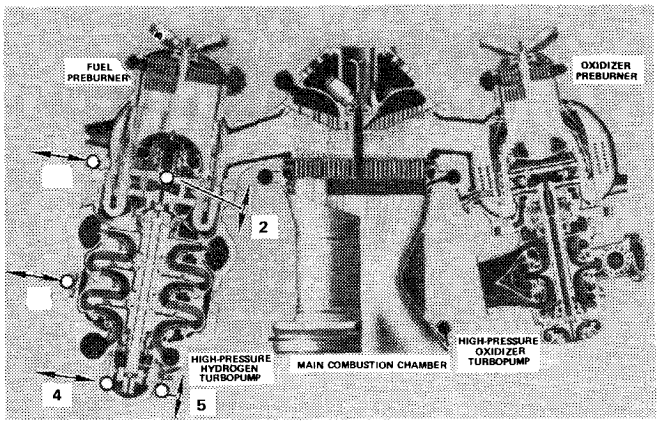

Fig. 4 Main powerhead arrangement showing accelerometer locations on HPFTP casing (arrows indicate direction of accelerometer sensitivity).

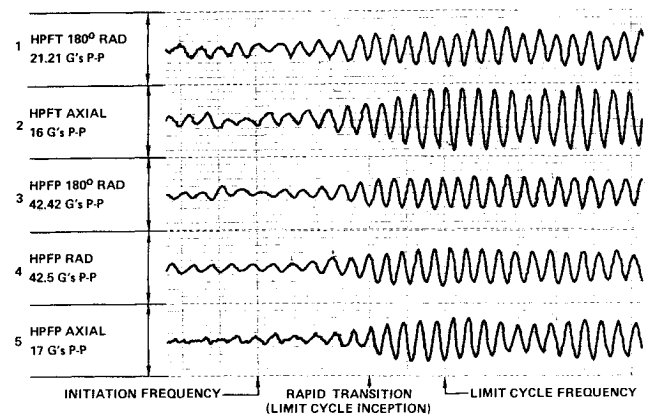

Fig. 5 Typical whirl initiation and limit cycle characteristics.

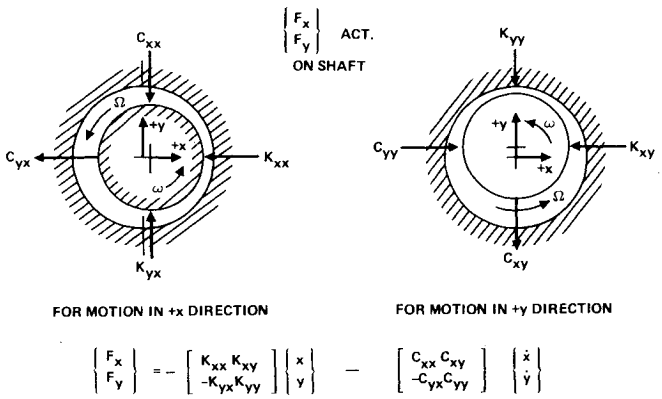

$$\begin{Bmatrix} F_x \\ F_y \end{Bmatrix} = -\begin{bmatrix} K_{xx} & K_{xy} \\ -K_{yx} & K_{yy} \end{bmatrix} \begin{Bmatrix} x \\ y \end{Bmatrix} - \begin{bmatrix} C_{xx} & C_{xy} \\ -C_{yx} & C_{yy} \end{bmatrix} \begin{Bmatrix} \dot{x} \\ \dot{y} \end{Bmatrix}$$

Fig. 6 Seal dynamic characteristics and sign convention.

Representation of Seal Effects

Although some stiffness change effects due to shaft/seal angularity resulting from shaft bending was hypothesized by Northern Research,[38] all models used some variant of the seal stiffness, damping, and cross-coupling effects proposed by Black.[8-18] Seal dynamic characteristic sign conventions and nomenclature are shown in Fig. 6. Representative dynamic values for various sealing points in the original baseline HPFTP are shown in Table 3 (see Jackson[34]). These effects were not only one of the important candidate drivers, but offered the only practical potential of introducing system damping. It is clear that the interstage seals(nos. 3 and 6 in Fig. 1) are dominant. Figure 7 shows the characteristics of various interstage seal configuratons which were manufactured. No. 1 is the original basic, serrated interstage seal; no. 2 is an attempt to destroy the cross-coupling (pumping) effects without increasing seal leakage; no. 3 accepts increased seal leakage while reducing all seal forces to a minimum; while nos. 4 and 5 deliberately build up all of the important seal terms with the vitally important idea that the beneficial stiffness and damping terms will outstrip the cross-coupling terms in the total system.

Considerable controversy attended the selection of these seal values, and it is not known even at present how accurate they may be. Black's data, for example, was obtained at a Reynolds number of 20,000, while the seals in the HPFTP operate at numbers as high as 500,000.

Alford Effects

Aerodynamic cross-coupling at the turbine was assumed in all models to be consistent with that proposed by Alford[32]

$$K_t = \tau\beta / D_p H$$

where τ is the turbine torque, H is the blade height, and β is the change of efficiency per unit of rotor displacement. Alford recommended $\beta = 1.5$ for our case, although much larger values, such as 8, were used by Gunter[5] for exploratory purposes. This effect was deemed to be a major source of instability, particularly in the presence of the low system stiffness of the baseline system.

Internal Shaft Hysteresis, Bearing Support, Casing Stiffnesses, and Bearing Stiffness

Load deflection tests confirmed shaft predicted stiffness within 4%. These and shaker tests confirmed the natural frequency of the shaft within 5%. The equivalent hysteresis of the shaft was equal to 0.6% of critical damping for the first free/free mode. Spring rates of the bearing carriers are shown in Fig. 3 and are approximated as piecewise nonlinear. Spring rates of the casing are shown in Fig. 8 and were within 25% of the predicted value. In general, measured spring rates of structures in excess of 1×10^6 lb/in. were lower than predicted and difficult to measure accurately.

The bearing stiffness prediction, shown in Fig. 9, is a function of speed, and is derived from a program by Jones.[39]

Effects of Testing Various Design Modifications

Early analysis indicated a stabilizing effect would be achieved if system stiffness and damping at the bearings were both increased. Apparent effective stiffness was also adversely influenced by bearing deadband. To increase shaft stiffness and reduce internal hysteresis, shaft collar diameters 3, 6, and 8 (Fig. 1) were increased and the central drawbolt tension was maximized. Additional Belleville springs were added at position "B" (Fig. 3) in an attempt to increase support damping. Various seal designs were tested in sequence; these and the parameters associated with them are shown in Fig. 7. The result of introducing the system changes is shown in Fig. 10. The shaft speed at which initiation of whirl (ω_I) was detected is plotted against whirl frequency Ω. Line A is $\omega_I/\Omega = 2.5$ and line B is $\omega/\Omega = 2$, where ω is shaft speed. For the lowest system stiffness (the original system), the whirl frequency is ~135 Hz and the inception occurs at twice the first-critical speed, while for the stiffener systems, e.g., multiple tight Bellevilles, tight clearances, and stiff shaft, the inception lies along line A, but jumps within a few milliseconds to line B. As the system was progressively stiffened by adding more Belleville washers, tight caps (no. 2, Fig. 3), etc., the data points moved to the right as the first-critical speed was increased. Although the various Bellevilles may have added some damping, the principal effect seems to have been to progressively, and in some cases, erratically stiffen the system. Very stiff bearing supports (no. 3, Fig. 3) tended toward line B at higher frequencies. It is believed that, for the data in Fig. 10, $\Omega = \omega_{cr}$.

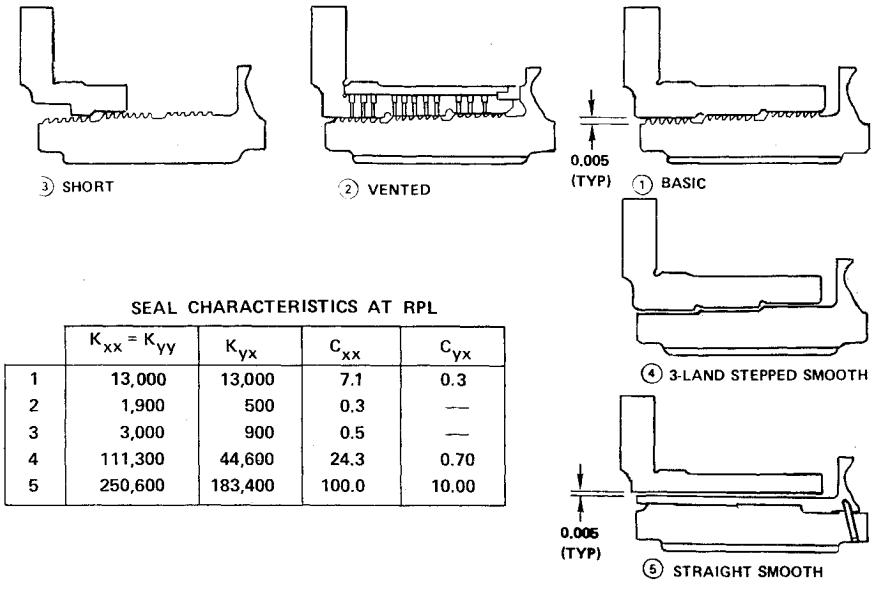

Fig. 7 Dynamic characteristics of various seal designs compared to the basic design.

SEAL CHARACTERISTICS AT RPL

	$K_{xx} = K_{yy}$	K_{yx}	C_{xx}	C_{yx}
1	13,000	13,000	7.1	0.3
2	1,900	500	0.3	—
3	3,000	900	0.5	—
4	111,300	44,600	24.3	0.70
5	250,600	183,400	100.0	10.00

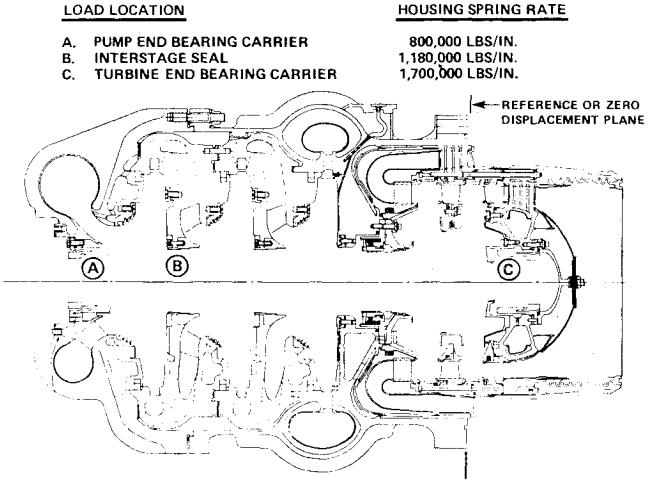

Fig. 8 HPFTP casing stiffness.

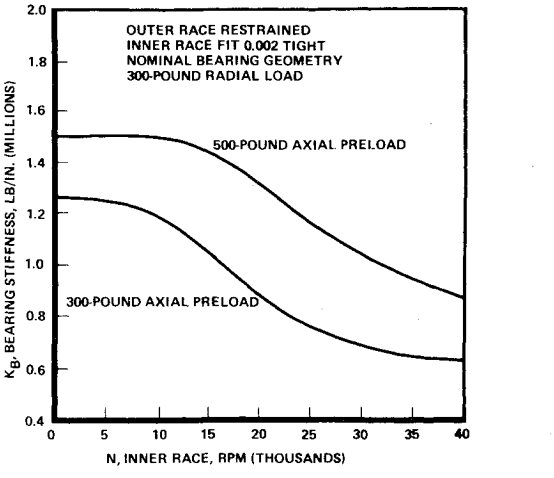

Fig. 9 Radial stiffness of ball bearing as a function of axial preload and shaft speed.

Subsequent to this testing and supported by computer analysis, the stepped smooth and straight smooth interstage seals (Fig. 7) were introduced at diameters 3 and 6 (Fig. 1), and whirl was reduced to such a low level as to be barely preceptible. When adequate cooling was finally supplied to the turbine bearing to solve a bearing overheating problem, even this low-level whirl disappeared, perhaps as a result of hydrogen entering the bearing clearances.

Although much augmented spring rate and damping characteristics were predicted for the straight smooth seal, no discernible difference was seen as a result of test in comparison with the stepped smooth seal. Because of concern over building up redundant bearing loads in the event of seal and bearing misalignment, together with increased interstage leakage, the stepped smooth seal was selected rather than the straight smooth for the final configuration. For nondamaged hardware, whirl has been absent within the operating range.

The rationale for the success of the configuration through the duplication of test results on the computer will now be addressed.

Results of Analysis

Although there were some early quantitative disagreements in the model results, there was eventual general agreement between models on the following salient points:

1) Increasing the system damping tends to stabilize the system. Considerable increases are required to achieve stability with support damping alone (see Figs. 11 and 12).

2) Rotating internal hysteresis is a destabilizing influence, but is minor compared to turbine cross-coupling, seal, and possible other effects for the amount of rotor internal hysteresis identifiable by test ($\xi = 0.6\%$).

3) Casing modes are not a major factor in causing instability because of the wide separation between the lowest casing modes and the instability frequencies.

4) Smooth interstage seals are a major stabilizing influence, and a straight smooth interstage seal is more effective than a stepped smooth interstage seal.

5) The stiffening and damping effects of the seals are not fully realized until high shaft speeds ($\omega > 25{,}000$ rpm) are attained; therefore, it was important to raise the first system critical to a maximum; this increases with shaft speed (see Fig. 13).

6) Rotor sideloads and offset seals are stabilizing influences.

7) All models indicated that asymmetric bearing support stiffnesses were a stabilizing influence.

8) "Deadband," or clearance between bearing outer race and bearing carrier, is a destabilizing influence and causes reduction in apparent critical speeds.

9) There were significant interactions between effects, particularly seal forces, deadband, and sideloads.

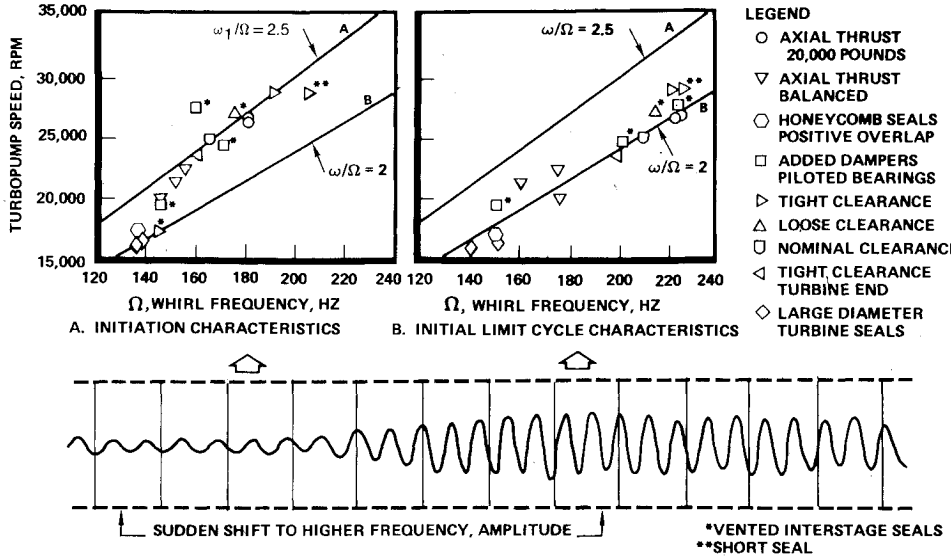

Fig. 10 HPFTP whirl characteristics for various configuration changes.

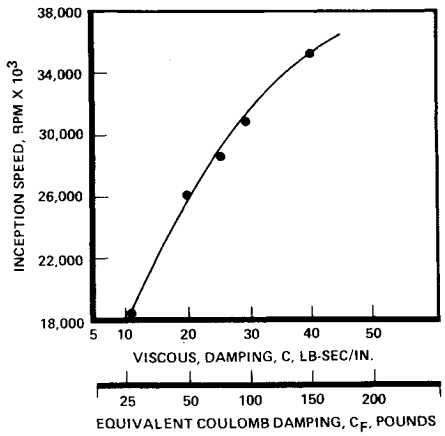

Fig. 11 HPFTP whirl inception vs support damping, nonlinear supports (Rowan).

It was found that the linear models, while valuable in indicating trends, were indifferently satisfactory in duplicating engine results.

With the nonlinear hybrid model, it was possible to duplicate engine behavior over a wide range of operating conditions. For example, in Fig. 14, the inception, limit cycle, and dropout behavior of four engine runs were duplicated over the corresponding range of system stiffness and hardware changes. An example of a comparison of test data with a computer run (901-045) is shown in Fig. 15; pre- and post-inception accelerometer frequencies and amplitudes match. It was unusual, however, to be able to predict with even the best model the behavior of the next engine run. This was due in part to an imperfect knowledge of exact tolerances in any given turbopump buildup and the uncertainties connected with the nonlinearities of the system. An example of this sensitivity is shown in Fig. 16. The effect of bearing deadband on the apparent second-critical speed is marked, and the effect of unbalance distribution in exiting the second critical as the greatest response is shown. The effect of degree of unbalance on both stability and apparent critical speed was also noted. In general, a large unbalance tended to postpone inception, but caused a more sudden and violent oscillation when subsynchronous vibration occurred. This phenomenon has been previously noted by other investigators such as Kushul'.[3]

Sideloads were a stabilizing influence with large values postponing inception. This effect has been noted by Hori.[2]

Perhaps the most important conclusion reached by the analysis process was that resulting from a careful study of the seal coefficients. This showed that the beneficial effects of spring rate and damping outstrip the destabilizing effects if the undamped natural frequency of the system can be increased beyond a critical value and the seals are stepped smooth, or even better, straight smooth. In effect, the first system critical is moved upward as speed increases, as is damping, to the extent that instability does not occur within the operating range.

The effect of asymmetrical bearing support stiffness was investigated as a possible stabilizing influence and was found to be most effective for large ratios of K_x to K_y. There was a strong effect of bearing support deadband on both first and

Table 4 Stability analysis summary

Hardware configuration						
Shaft	Seals	Pump support stiffness (K), lb/in.	Turbine support stiffness (K), lb/in.	Pump damping, lb-s/in.	Turbine damping, lb-s/in.	Onset speed of instability, rpm
Original	Original labyrinth	150,000	150,000	5	5	18,000
Original	3-land smooth	1,000,000	1,000,000	5	5	38,600
Stiff	3-land smooth	1,000,000	1,000,000	5	5	40,500
Stiff	Straight smooth	1,000,000	1,000,000	5	5	47,500
Stiff	Hydrostatic	1,000,000	1,000,000	5	5	>50,000
Stiff	Straight smooth + turbine	1,000,000	1,000,000	5	5	49,500
Stiff	Straight smooth	200,000	1,000,000	20	5	45,000
Stiff	Straight smooth	132,000/374,000	132,000/374,000	5	5	43,000
Stiff	Straight smooth	132,000/374,000	1,000,000	20	5	47,600
Stiff	Stepped smooth	132,000/374,000	1,000,000	20	5	>50,000

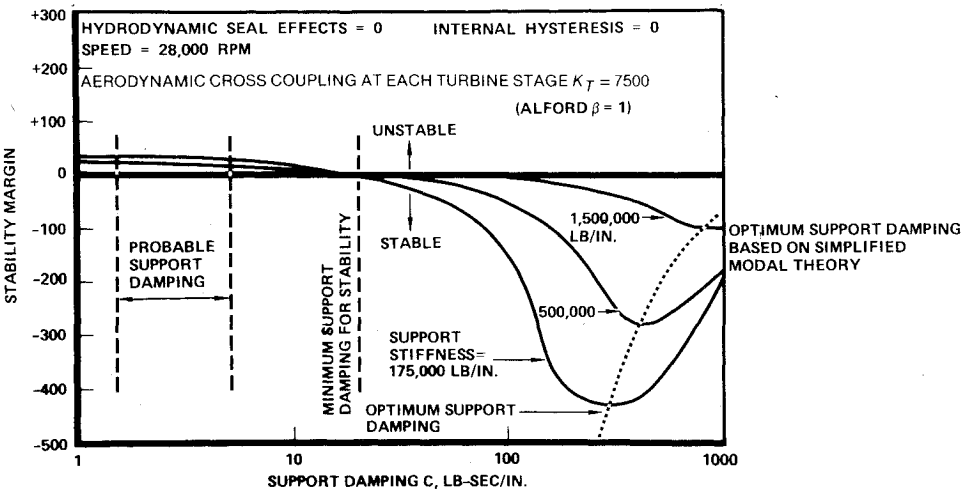

Fig. 12 HPFTP whirl stability margin as a function of support damping and stiffness (Gunter).

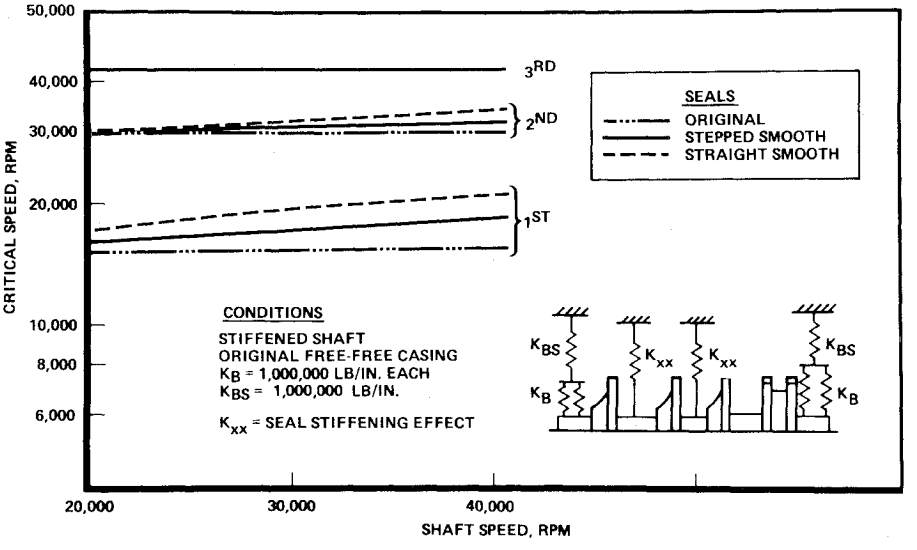

Fig. 13 Effect of various seal configurations upon the critical speeds of the stiffened system (Rowan).

second critical speeds (see Fig. 17) for stiff systems. This was deemed insignificant in the flexible baseline system.

Table 4 summarizes the stability of the baseline configuration with various system configurations. For satisfactory operation, a stiff shaft, bearing carrier, and at least the three-land stepped smooth seal are required for stable operation.

Conclusions

For this specific problem, the salient conclusions to be drawn are:

1) The most important drivers or forcing functions were the hydrodynamic cross-coupling of the numerous seals, the interstage seals being the most important, the aerodynamic cross-coupling of the two turbine stages (the Alford effect), and the possible participation of impeller/diffuser interaction (Ref. 10), although this effect is quantitatively uncertain. The above effects combined with low system stiffness to produce the instability. Other candidate forcing functions, such as internal hysteresis, can be regarded as secondary.

2) The most important stabilizing effects were the increase of system stiffening and damping afforded by the incorporation of stepped smooth seals, together with an increase of bearing support and shaft stiffness. These actions have moved the system instability beyond the present operating range. Increase of seal clearances by rubbing interference or loss of bearing support stiffness has occasionally permitted whirl to recur.

3) Additional pump design parameters which may affect stability inception were identified as a result of analysis, e.g., bearing race deadband or clearance, unbalance, impeller sideloads, and nonlinearity. The influence of these, in general, can be regarded as affecting the speed at which inception occurs and its relative violence in a system already susceptible to whirl because of other factors.

4) Friction damping at bearing supports was ineffectual and erratic. Some computer work by Shen[34] indicates that under certain conditions friction damping may indeed be a destabilizing effect. This type of damping must be termed highly questionable for fundamental design. Metal mesh dampers were fabricated, but not incorporated.

General Observations

Computer Modeling

Computer models are of great utility in pointing the way to solutions, but suffer from a lack of really definitive data on many of the key forcing functions. For this problem, linear models gave general trends, and more complex nonlinear models eventually matched the behavior of the HPFTP. But in general, even after extensive test/model matching, the results of any given upcoming test could not be predicted with accuracy by computer.

Much more work needs to be done on the dynamic behavior of high-pressure drop seals over a wide range of Reynolds numbers, the Alford effect, impeller/diffuser cross-coupling, and the effects of bearing deadband all in a nonlinear environment.

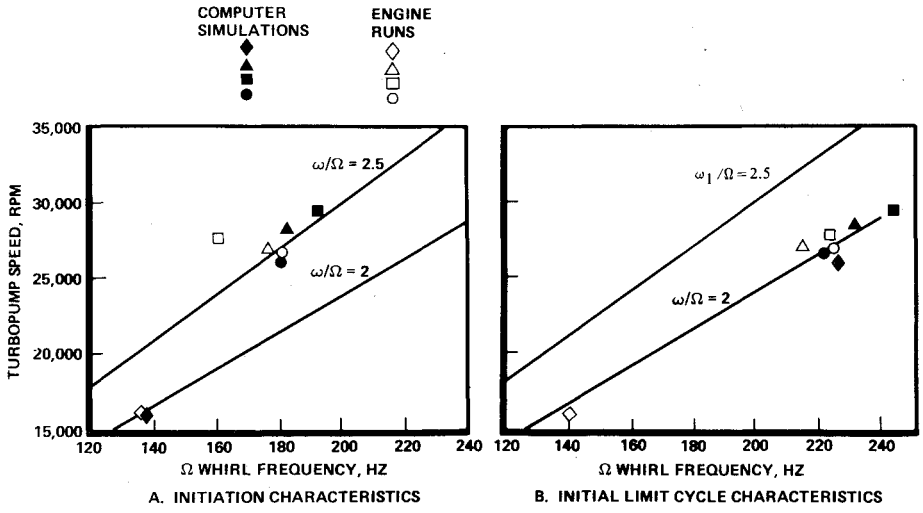

Fig. 14 Nonlinear hybrid model simulations compared to engine runs (Thompson, Biggs).

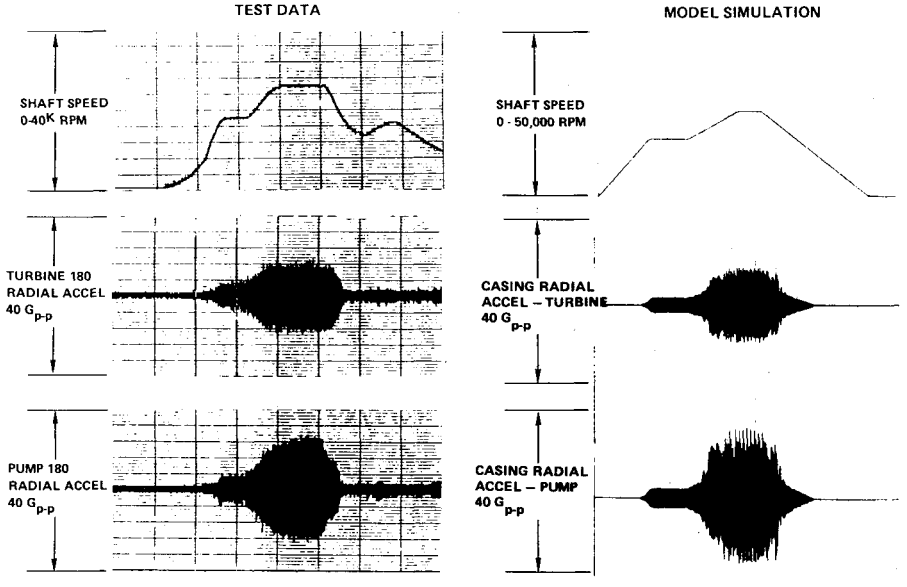

Fig 15 Acceleration vs time comparison of ISTB test 901-045 with hybrid computer model test run (Thompson, Biggs).

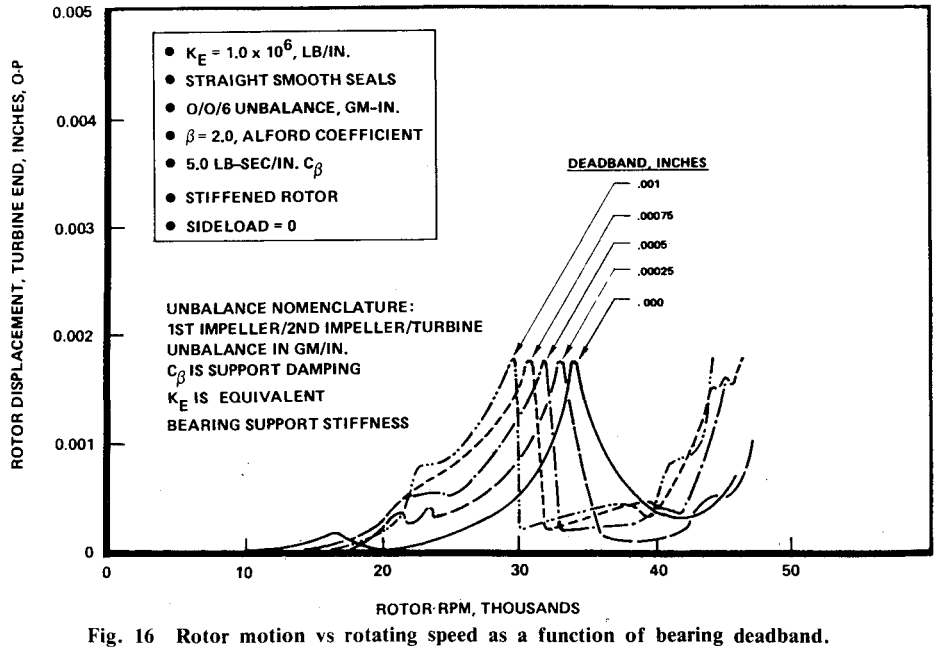

Fig. 16 Rotor motion vs rotating speed as a function of bearing deadband.

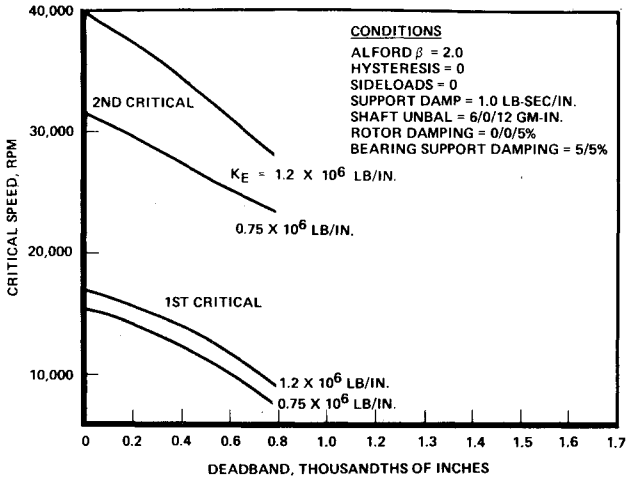

Fig. 17 Effect of bearing support deadband on the first two critical speeds for a stiffened shaft with straight smooth seals (Sack).

Aspects of Machine Design

This problem was solved with no direct information regarding shaft behavior, this being inferred from casing accelerometer data, bearing and seal appearance, and computer calculations. New machinery should be designed so that noncontacting proximity pickups can be readily installed to directly indicate the relationship of the shafting to the casing in the event of a problem.

Analysis and Design of New Machines

Although much progress has been made in the field of stability analysis of high-speed rotating machinery, sizable calculated margins should be shown on new designs and a healthy skepticism should prevail during the design and development program. Turbine blades should be shrouded if possible, the minimum number of pilots should be employed on shafting, seals with high-pressure drops should have cylindrical close-fitting elements if leakage permits, and provision should by made at all possible shaft locations for the introduction of additional damping if required.

Acknowledgments

Acknowledgment is here made of contributions by many individuals at NASA, Rocketdyne, other manufacturers, and the academic community for information and work delineated in this paper. Many of these are mentioned by name in the references. All work was sponsored by the NASA Marshall Space Flight Center, Huntsville, Alabama, under Contract NAS8-27980.

References

[1] Rothe, K., "Turbopump Configuration Selection for the Space Shuttle Main Engine," ASME Paper 74-FE-23, Joint Fluid Engineering Conference, Montreal, Canada, May 1974.

[2] Hori, Y., "A Theory of Oil Whip," Paper 59-APM-2, ASME Applied Mechanics Division, Feb. 1958.

[3] Kushul', M.Y., *The Self-Induced Oscillations of Rotors*, Consultants Bureau, New York, 1964, p. 102.

[4] Bolotin, V.V., *Nonconservative Problems of the Theory of Elastic Stability*, Macmillan, New York, 1963, pp. 139-186.

[5] Gunter, E.J., Jr., Allaire, P.E., et al., *The Dynamic Analysis of the Space Shuttle Main Engine High-Pressure Fuel Turbopump* (in five volumes), University of Virginia, Report No. ME-4012-101-76, 528140/ME76/102, 103, 104, June-Sept. 1976.

[6] Creslein, W. (Pratt & Whitney Aircraft) and Goetz, O., (NASA MSFC), personal communication, 1976.

[7] Childs, D.W., *Transient Rotordynamic Analysis for the Space Shuttle Main Engine High-Pressure Turbopumps*, 1973 ASEE-NASA Summary Faculty Fellowship Program Final Report, University of Alabama, 1973.

[8] Black, H.F., "The Stabilizing Capacity of Bearings for Flexible Rotors with Hysteresis," *Transactions of the ASME*, Paper 75-DET-55, Sept. 1975.

[9] Black, H.F., "Effects of Hydraulic Forces in Annular Pressure Seals on the Vibrations of Centrifugal Pump Rotors," *Journal of Mechanical Engineering Science*, Vol. 11, No. 2, 1969, pp. 206-213.

[10] Black, H.F., "Calculation of Forced Whirling and Stability of Centrifugal Pump Rotor Systems," *Transactions of the ASME*, Paper 73-DET-131, Sept. 1973, pp. 92-100.

[11] Black, H.F. and Jennssen, D.N., "Dynamic Hybrid Bearing Characteristics of Annular Controlled Leakage Seals and Pressure Seals," *Proceedings of the Institution of Mechanical Engineers*, Vol. 184, Pt. 3N, Sept. 1970, pp. 92-100.

[12] Black, H.F., "Lateral Stability and Vibrations of High Speed Centrifugal Pump Rotors," *Dynamics of Rotors Symposium*, Lyngby/Denmark, 1975, edited by F.I. Niordson, Springer-Verlag, pp. 57-74.

[13] Black, H.F., "Effects of Hydraulic Forces in Annular Pressure Seals on the Vibrations of Centrifugal Pump Rotors," *Journal of Mechanical Engineering Science*, Vol. 11, No. 2, 1968, pp. 206-213.

[14] Black, H.F. and Jennssen, D.N., "Dynamic Hybrid Bearing Characteristics of Annular Controlled Leakage Seals," *Proceedings of the Institution of Mechanical Engineers*, Vol. 184, Pt 3N, 1969-70, pp. 92-100.

[15] Black, H.F. and Jennssen, D.N., "Effects of High-Pressure Ring Seals on Pump Rotor Vibrations," Paper 71-WA/FE 38, American Society of Mechanical Engineers, Nov. 28-Dec. 2, 1971.

[16] Black H.F. and Cochrane, E.A., "Leakage and Hybrid Bearing Properties of Serrated Seals in Centrifugal Pumps," 6th International Conference on Fluid Sealing, Munich, German Federal Republic, Feb. 27-March 2, 1973.

[17] Black, H.F., "On Journal Bearings with High Axial Flows in the Turbulent Regime," Research Notes, *Journal of Mechanical Engineering Science*, Vol. 12, No. 4, 1970, pp. 301-303.

[18] Black, H.F., "Lateral Stability and Vibrations of High-Speed Centrifugal Pump Rotors," Department of Mechanical Engineering, Heriot-Watt University, Edinburgh, United Kingdom, 1975.

[19] Gunter, E.J. Jr., "Dynamic Stability of Rotor-Bearing Systems," NASA SP-113, 1966.

[20] Gunter, E.J. Jr., Barrett, L.E., and Allaire, P.E., "Design and Application of Squeeze Film Dampers for Turbomachinery Stabilization," *Proceedings of the Fourth Turbomachinery Symposium*.

[21] Gunter, E.J. Jr. and Trumpler, P.R., "The Influence of Internal Friction on the Stability of High Speed Rotors With Anisotropic Supports," *Journal of Engineering for Industry*, Vol. 91, Nov. 1969, p. 1105.

[22] Kirk, R.G. and Gunter, E.J. Jr., "Nonlinear Transient Analysis of Multi-Mass Flexible Rotors—Theory and Applications," NASA CR-2300, Sept. 1973.

[23] Lund, J.W. and Saibel, E., "Oil Whip Whirl Orbits of a Rotor in Sleeve Bearings," *Journal of Engineering for Industry*, Paper 67-Vibr-28, Nov. 1967, pp. 813-823.

[24] Larson, R.H. and Richardson, H.H., "A Preliminary Study of Whirl Instability for Pressurized Gas Bearings," *Journal of Basic Engineering*, Dec. 1962, pp. 511-520.

[25] Landzberg, A.H., "Stability of a Turbine-Generator Rotor Including the Effects of Certain Types of Steam and Bearing Excitations," *Journal of Applied Mechanics*, Sept. 1960, pp. 410-416.

[26] Gross, W.A., "Investigation of Whirl in Externally Pressurized Air-Lubricated Journal Bearings," *Transactions of the ASME*, Paper 61 Lub-1, March 1962, pp. 132-138.

[27] Ehrich, F.F., "Shaft Whirl Induced by Rotor Internal Damping," *Journal of Applied Mechanics*, June 1964, pp. 279-282.

[28] Ehrich, F.F. and O'Connor, J.J., "Stator Whirl with Rotors in Bearing Clearance," *Journal of Engineering for Industry*, Aug. 1967, pp. 381-390.

[29] Elwell, R., "Energy Theory of Half-Frequency Whirl," *Journal of Basic Engineering*, Sept. 1961, pp. 478-480.

[30] Crandall, S.H. and Brosens, P.J., "On the Stability of Rotation of a Rotor with Rotationally Unsymmetric Inertia and Stiffness Properties," *Journal of Applied Mechanics*, Dec. 1961.

[31] Poritsky, H., "Rotor Stability," *U.S. National Congress of Applied Mechanics*, 1966, pp. 37-61.

[32] Alford, J.S., "Protecting Turbomachinery from Self-Excited Rotor Whirl," *Journal of Engineering for Power*, Oct. 1965, pp. 333-344.

[33] Tondl, A., *Some Problems of Rotor Dynamics*, Chapman & Hall, London, England, 1965.

[34] Unpublished Rocketdyne reports and presentations by the following individuals on itemized subjects. All work conducted under NASA Contract NAS8-27980, April-Dec. 1976: a) Biggs, R.E., "Correlation of Engine Dynamic Data on the HPFTP"; b) Ek, M.C., various presentations to NASA officials from April-Aug. 1976; c) Jackson, E.D., "Integration of Hydrodynamic Seal Effects on the HPFTP"; d) Rowan, B.R., "Digital Computer Representation of the Critical Speeds of the HPFTP," and "Digital Real Time Stability and Response Model of the HPFTP"; e) Sack, L.E., Farrel, E.C., and Rowan, B.R., "Real Time Hybrid Computer Stability Model of the HPFTP"; f) Shen, F.A., "Analytical Representation of Various Coulomb Internal Hysteresis Models of the HPFTP"; g) Thompson, J.L. and Biggs, R.E., "Intercorrelation of Various Computer Models With Computer Data of the HPFTP"; h) Yu, Y. Y., "Several Mathematical Analyses Resulting from a Study of the Literature."

[35] Childs, D.W., "The Space Shuttle Main Engine High-Pressure Fuel Turbopump Rotordynamic Instability Problem," ASME Paper 77-GT-49, Gas Turbine Conference, Philadelphia, Pa., March 1977.

[36] Rowan, B.R., Sack, L.E., and Farrel, E.C., "Space Shuttle Main Engine Rotor Dynamics Simulation," presented at the Society for Computer Simulation, Los Angeles, Calif., May 4, 1977.

[37] Goetz, O., Worley, H.E., et al., Numerous reports and presentations on the rotor instability of the HPFTP, mathematical models, tests, hardware considerations. Unpublished internal material at NASA/MSFC, Ala., in connection with NASA Contract NAS8-27980.

[38] "Pump Rotor System Whirl Forcing Analysis," Northern Research & Engineering Company, Cambridge, Mass., Report No. 950-446, May 1976.

[39] Jones, A.B., "A General Theory for Elastically Constrained Ball and Radial Roller Bearings under Arbitrary Load and Speed Conditions," *ASME Journal of Basic Engineering*, Paper 59-Lub-10, V. 82, June 1960, p. 309.